



Cite this: *Phys. Chem. Chem. Phys.*,
2017, **19**, 32733

Received 4th July 2017,
Accepted 23rd November 2017

DOI: 10.1039/c7cp04474g

rsc.li/pccp

Protonation of N₂O and NO₂ in a solid phase†

Evgenii S. Stoyanov^{id}*^{ab} and Irina V. Stoyanova^a

Adsorption of gaseous N₂O on the acidic surface Brønsted centers of the strongest known solid acid, H(CHB₁₁F₁₁), results in formation of the N≡N–OH⁺ cation. Its positive charge is localized mainly to the H-atom, which is H-bonded to the CHB₁₁F₁₁[−] anion forming an asymmetric proton disolvate of the L₁–H⁺⋯L₂ type, where L₁ = N₂O and L₂ = CHB₁₁F₁₁[−]. NO₂ protonation under the same conditions leads to the formation of the highly reactive cation radical NO₂H^{•+}, which reacts rapidly with an NO₂ molecule according to the equation N₂OH⁺ + NO₂ → [N₂O₄H⁺] → N₂OH⁺ + O₂ resulting in the formation of two types of N₂OH⁺ cations: (i) a typical Brønsted superacid, N≡N–OH⁺, with a strongly acidic OH group involved in a rather strong H-bond with the anion, and (ii) a typical strong Lewis acid, N≡N⁺–OH, with a positive charge localized to the central N atom and ionic interactions with the surrounding anions *via* the charged central N atom.

Introduction

Weakly basic small molecules H₂, N₂, O₂, CO₂, CO, N₂O, NO₂ are interesting targets for protonation. No evidence has been obtained for the protonation of these simple gaseous molecules under ambient conditions in a “magic” superacid system, HSO₃F–SbF₅–SO₃,¹ one of the strongest known mixed Brønsted/Lewis acids. Nonetheless, a somewhat stronger HF/SbF₅ mixed acid system can protonate CO, when it is dissolved, but under conditions of high pressure (up to 85 atm).^{2,3} The corresponding salt is not isolable. Using a newly synthesized strongest solid superacid, H(CHB₁₁F₁₁),⁴ we have been able to protonate CO under ambient conditions both through the C atom and *via* the O atom and to obtain in preparative quantities bulk salts of the H⁺CO and COH⁺ cations.³ Therefore, the H(CHB₁₁F₁₁) acid manifests itself as stronger than the “magic” acids, and is expected to protonate (under ambient conditions) other, less basic than CO, molecules such as N₂O and NO₂, which still cannot be protonated in a condensed phase. In a gas phase, the protonation of small molecules was proved by mass spectroscopy^{5–10} and IR spectroscopy.^{11–13} For example, N₂O is protonated *via* the O atom, and the frequency of the O–H⁺ stretch was found to be 3331 cm^{−1} for the gas phase,^{12,13} and 43.3 cm^{−1} lower for the Ne matrix.¹⁴ The experimental difficulties with the protonation of the simple molecules are compensated so far by the research in this field on the basis of quantum-chemical calculations,^{15–24}

that confirmed that the O-protonated isomer (NNOH⁺) is energetically more preferable (by 4.02 kcal mol^{−1})²⁴ than the N-protonated isomer.

Recently, it was reported²⁵ that CO₂ is protonated by H(CHB₁₁F₁₁) with the formation of a stable (at room temperature) salt of the symmetric disolvate OCO–H⁺–OCO. This seems unexpected because CO, being more basic than CO₂, forms under the same conditions only salts of the L₁–H⁺⋯L₂ type cations with an asymmetric bridged proton, where L₁ = CO and L₂ = CHB₁₁F₁₁[−] anion.³ The basicity of CO is not sufficient to substitute L₂ for the formation of symmetric OC–H⁺–CO. It is interesting to test whether other weakly basic molecules, N₂O or NO₂, can form the symmetric disolvates L–H⁺–L. Moreover, the carborane salts of the protonated nitrogen oxides must have superacidic properties, as salts of the COH⁺ cation,³ and can serve as the reagents for obtaining new types of functionalized carbocations.

In the present work, we studied the protonation of N₂O and NO₂ by the strongest known solid carborane superacid, H(CHB₁₁F₁₁) (Fig. 1), using the methods of infrared (IR) spectroscopy and quantum chemistry.

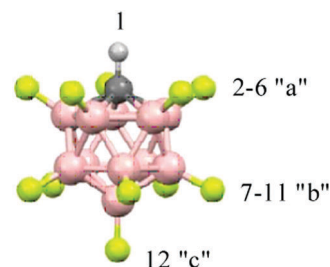


Fig. 1 Icosahedral carborane anions, CHB₁₁F₁₁[−], with the numbering of three types of F atoms differing in basicity.

^a Vorozhtsov Institute of Organic Chemistry, Siberian Branch of Russian Academy of Sciences, Novosibirsk 630090, Russia. E-mail: evgenii@nioch.nsc.ru

^b Department of Natural Sciences, National Research University – Novosibirsk State University, Novosibirsk 630090, Russia

† Electronic supplementary information (ESI) available. See DOI: 10.1039/c7cp04474g



Experimental

Carborane acid $\text{H}(\text{CHB}_{11}\text{F}_{11})$ hereafter abbreviated as $\text{H}\{\text{F}_{11}\}$ was prepared as previously described.⁴ IR spectroscopic analysis of the interaction of N_2O or NO_2 with $\text{H}\{\text{F}_{11}\}$ was performed as follows. The solid acid was sublimed at 150–160 °C under a pressure of 10^{-5} Torr on cold Si windows in a specially designed IR cell reactor, forming a very thin translucent film of the amorphous acid.³ Dry gaseous N_2O or NO_2 (obtained from Sigma Aldrich, 99% purity), was injected anaerobically into the IR cell inside a dry box and reacted with the acid at room temperature. IR spectra were recorded at certain time intervals. Weighable amounts of the $\text{N}_2\text{OH}^+\{\text{F}_{11}^-\}$ salt were obtained by aging of a portion of $\text{H}\{\text{F}_{11}\}$ for 1 day in a Schlegel tube filled with N_2O .

All procedures were performed in a Spectro-systems glove-box under an atmosphere of Ar ($\text{H}_2\text{O} < 1$ ppm). The IR spectra were recorded on an Bruker Vector 22 spectrometer inside a dry box in either transmission or attenuated total reflectance (ATR) mode (525–4000 cm^{-1}). The IR data were processed with the GRAMMS/A1 (7.00) software from Thermo Fisher Scientific.

Computational details

The geometric parameters of the species under study were optimized at the B3LYP-D3/def2-TZVPD level of theory^{26–29} with an ultrafine grid. The equilibrium structures of the specific compounds were also calculated in a dichloroethane (DCE) solution using the SMD solvation model.³⁰ All stationary points were characterized as minima by a vibrational analysis (the number of imaginary frequencies was equal to zero). Zero-point energies were computed from the corresponding vibrational frequencies without scaling factors. (SMD)-B3LYP-D3/def2-TZVPD optimized structures were used in all subsequent computations.

To compare the calculated and experimental vibrational frequencies, the (SMD)-B3LYP-D3/def2-TZVPD harmonic frequencies were scaled by the factor of 0.9674 as recommended by Kesharwani *et al.*³¹ Although application of the scaling factor to the highly anharmonic NH and OH stretch vibrations requires caution: a high-accuracy *ab initio* anharmonic force field study of N_2OH^+ showed²³ that for the purposes of this work, the above mentioned scaling of the harmonic frequencies is reasonable. To obtain more accurate relative energies of some isomers, single-point high-level CCSD(T)/def2-TZVPD coupled-cluster computations³² within a frozen core approximation were additionally conducted.

The natural population analysis partial charges^{33,34} were calculated at the (SMD)-B3LYP-D3/def2-TZVPD theoretical level for the species of interest as implemented in Gaussian09,³⁵ whereas natural resonance theory^{36–38} analysis was carried out at the B3LYP/TZ2P level of theory using scalar relativistic (SR) zero-order regular approximation Hamiltonian (core potentials were not used, and the quality of the Becke numerical integration grid was set to the keyword good)³⁹ in the ADF2016 software suite.^{40–42}

(SMD)-B3LYP-D3/def2-TZVPD and CCSD(T)/def2-TZVPD computations were performed using the Gaussian09 software.³⁵ The def2-TZVPD basis sets were retrieved from the EMSL database.^{43,44}

All the compounds were assumed to be in their ground state. The spin-unrestricted formalism was used for both density functional theory (DFT) and CCSD(T) calculations when computing radicals.

Results of calculations

The gas phase B3LYP-D3/def2-TZVPD calculations of $\{\text{F}_{11}\}$ -containing compounds do not fully describe the ionic interactions taking place in the solid state, leading to a bad agreement between some calculated and experimental vibrational frequency values of the cations (Fig. S1–S3, ESI†). For this reason, we performed calculations for the $\text{N}_2\text{OH}^+\cdots\text{L}$ and $\text{NO}_2\text{H}^+\cdots\text{L}$ model systems, where L = Ar, Kr, Xe, CO, or SO_2 . A wide range of L basicities, which includes the basicity of the $\{\text{F}_{11}^-\}$ anion, allows us to interpret the experimental IR spectra more correctly (Fig. S4, ESI†). To model the effect of the environment playing an important role in crystals, we also conducted SMD-B3LYP-D3/def2-TZVPD calculations in a DCE solution for the compounds of interest (Fig. S5, ESI†).

(N_2O) H^+ cation

Protonation of N_2O is possible *via* terminal N and O atoms (Fig. S1, ESI†). The O-protonated structure is more stable (the energy difference between the O- H^+ and N- H^+ isomers is 3.9 kcal mol^{-1} at the CCSD[T]/def2-TZVPD//B3LYP-D3/def2-TZVPD level of theory; Fig. S1, ESI†), which is in line with other experimental¹² and theoretical studies.^{17–19,22–24}

N_2O described by the N-oxide valence formula, $\text{N}\equiv\text{N}^+-\text{O}^-$ (Fig. S6, ESI†), has two valence frequencies (Table S1, ESI†), $\nu_{\text{as}}\text{N}_2\text{O}$ at 2268 cm^{-1} and $\nu_{\text{s}}\text{N}_2\text{O}$ at 1285 cm^{-1} , which can be represented as the characteristic vibrations of the NN and NO stretches, respectively. The bent vibration is at 598 cm^{-1} . Protonation of N_2O leads to formation of the $\text{N}\equiv\text{N}-\text{OH}^+$ cation (Fig. S7a, ESI†), with a significant decrease in the NO stretch (~ 250 cm^{-1}) and an increase in the NN stretch (by ~ 90 cm^{-1} ; Table S2, ESI†) because the N–O and $\text{N}\equiv\text{N}$ bonds approach the common single and triple bond respectively.

According to vibrational analysis, the solvation of N_2OH^+ by Ar, Kr, or Xe weakened the OH bond and strengthened the NO bond (Table S2, ESI†). The dependence of the ν_{NO} frequency (reflecting the N–O strength) on the proton affinity (PA) of the noble gases (L) is linear (Fig. 2) confirming that the N–O stretch is highly characteristic because the (N_2O) H^+-L bond is ionic. Nevertheless, the analogous dependences for ν_{OH} and ν_{NN} frequencies deviate from the linear function to a greater extent with the greater basicity of L because a decrease in the frequency of OH^+ stretch and an increase in the frequency of the NN stretch result in their convergence with an enhancement of their interaction. This mixing becomes more notable when N_2OH^+ is solvated by the stronger bases, CO, SO_2 , and $\{\text{F}_{11}^-\}$, which formed a partially covalent bond with a cation. This situation leads to the formation of a rather asymmetric proton disolvate of the $\text{L}_1-\text{H}^+\cdots\text{L}_2$ type ($\text{L}_1 = \text{N}_2\text{O}$; $\text{L}_2 = \text{SO}_2$,



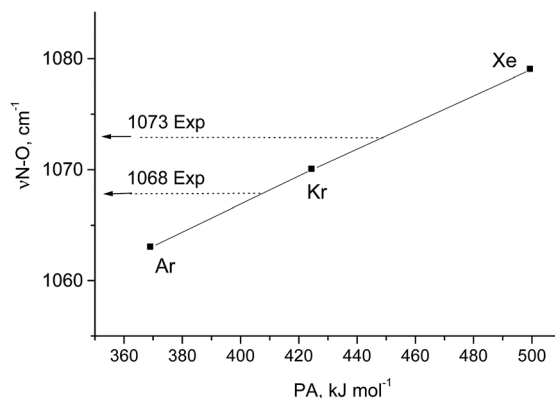


Fig. 2 Dependence of the N–O stretch of $\text{N}_2\text{O}-\text{H}^+\cdots\text{L}$ on the PA of L atoms. Experimental frequencies are given for comparison.

$\{\text{F}_{11}^-\}$) with a further increase in the frequency of the N–O stretch (Table S2, ESI[†]).

$(\text{NO}_2)\text{H}^+$ cation

The NO_2 molecule has two stretch vibrations, $\nu_{\text{as}}\text{NO}_2$ and $\nu_{\text{s}}\text{NO}_2$, with a frequency difference $\Delta = 295 \text{ cm}^{-1}$ (Table S1, ESI[†]). After protonation, the radical cation NO_2H^+ is formed (I.B.1 structure; Fig. S2, ESI[†]) having NO and NO(H) stretches with increased and decreased frequencies, respectively, as compared to NO_2 (Table S3, ESI[†]). Their difference Δ increased to 727 cm^{-1} indicating that the stretching vibrations acquire some characteristic nature. The solvation of $(\text{NO}_2)\text{H}^+$ with Ar decreases both NO stretches keeping their difference Δ actually unchanged. When the cation is solvated with stronger bases, Kr and Xe, the O–H⁺ bond continues to weaken (νOH^+ decreases), thus strengthening the N–O(H⁺) bond and its frequency (Table S3, ESI[†]). With a further increase in the basicity of L (CO, SO_2), H⁺ of $(\text{NO}_2)-\text{H}^+\cdots\text{L}$ became a typical bridged proton with stretch frequencies of $1500\text{--}1100 \text{ cm}^{-1}$.

$(\text{N}_2\text{O}_4)\text{H}^+$ cation

Gaseous NO_2 is always in equilibrium with N_2O_4 . Accordingly, the protonation of NO_2 may be accompanied by the protonation of N_2O_4 . The latter is unstable, which is related to the large N–N bond length of 1.78 \AA . After protonation, the optimized structure of $\text{N}_2\text{O}_4\text{H}^+$ (Ic10 in Fig. S4, ESI[†]) showed a significant increase in the N–N distance (2.247 \AA), which precluded its formation. Solvation of the $\text{N}_2\text{O}_4\text{H}^+$ cation with such bases as Ar, CO, SO_2 , or $\{\text{F}_{11}^-\}$, reduced the N–N distance down to 2.179 , 2.079 , 2.023 , and 1.909 \AA respectively, but it was still big enough for the cation to exist. Calculations predicted that unstable $\text{N}_2\text{O}_4\text{H}^+\cdots\text{L}$ can decompose in the simplest way into a $(\text{HNO}_3\cdots\text{NO}^+)\cdots\text{L}$ compound (Fig. S4, S5 and Tables S4, S5, ESI[†]). In any case, it is expected that the protonation of N_2O_4 will lead to subsequent secondary reactions.

Experimental results

N_2O interaction with the $\text{H}\{\text{F}_{11}\}$ acid

After injection of N_2O into the IR cell-reactor with the sublimed $\text{H}\{\text{F}_{11}\}$ acid, we started to register the IR spectra immediately. Subtraction from these spectra of the spectrum of gaseous N_2O revealed a weak band at 2231 cm^{-1} , which is very close to the νNN band at 2224 cm^{-1} of gaseous N_2O , but without the fine vibrational structure (Fig. 3). Obviously, this pattern denotes N_2O molecules absorbed by the acidic surface Brønsted centers of solid $\text{H}\{\text{F}_{11}\}$. After vacuum removal of the gaseous N_2O , the band at 2231 cm^{-1} persisted, but after fast heating up to $100 \text{ }^\circ\text{C}$ in a sealed vacuumed cell, this band disappeared and a weak spectrum of gaseous N_2O appeared. Therefore, N_2O molecules are indeed adsorbed to the surface Brønsted centers of the $\text{H}\{\text{F}_{11}\}$ acid, and this sorption is relatively strong.

With time, in the IR spectra, two narrow bands of NN stretches of N_2OH^+ cations appeared and grew in intensity: at 2363 cm^{-1} and at 2320 cm^{-1} (Fig. 3). They belong to cations

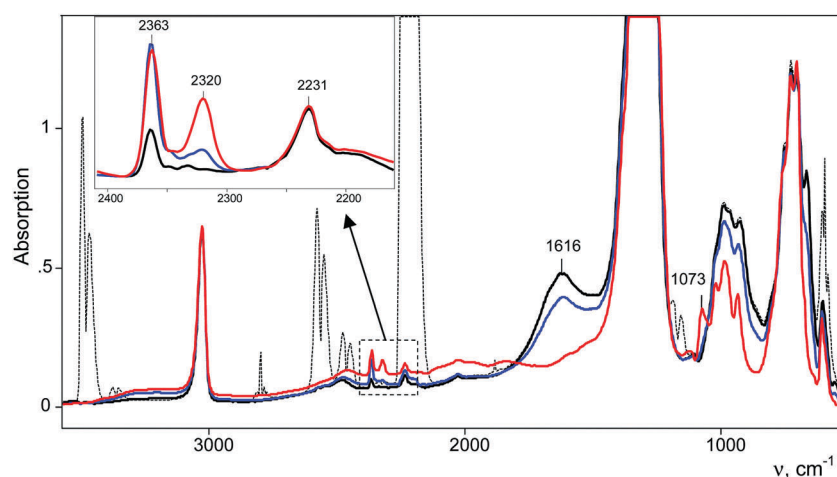


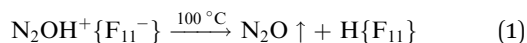
Fig. 3 IR spectra of the compounds formed when $\text{H}\{\text{F}_{11}\}$ is aged under an atmosphere of N_2O for 2 min (black solid and dashed curves), 1 h (blue curve) and 10 h (red curve). The spectra are shown before (dashed curve) and after subtraction (black solid curve) of the spectrum of gaseous N_2O . The red spectrum was registered after vacuum removal of the gaseous phase.



that bind to the most basic “b” and “c” sites of the $\{F_{11}^-\}$ anion (hereinafter referred to as $N_2OH^+_b$ and $N_2OH^+_c$), as is the case for H^+CO binding to $\{F_{11}^-\}$.³ Simultaneously, the absorption corresponding to the free (unreacted) $H\{F_{11}\}$ acid decreases and after 8–10 h disappears (judging by the indicative band at 1616 cm^{-1} of the stretch vibration of the bridged proton in polymeric acid $[H\{F_{11}\}]_n$, Fig. 3). In the low-frequency region of the $N-O(H^+)$ stretches, weak complex bands appeared at 1068 and 1073 cm^{-1} , which correspond to $N_2OH^+_c$ and $N_2OH^+_b$, respectively (Fig. 5).

Fig. 4 shows the intensity dependences of the bands of the NN stretches from $N_2OH^+_b$ and $N_2OH^+_c$ (A_{NN} at 2321 or 2364 cm^{-1} respectively) on the absorption intensity of the acid being used (an intensity decrease at 1616 cm^{-1} , A_{1616}). The figure shows that the formation of the $N_2OH^+_b$ and $N_2OH^+_c$ cations initially increased proportionally. Then, the filling of the most basic “c” site of $\{F_{11}^-\}$ reached saturation, while the filling of the “b” site continued.

The absorption corresponding to the $O-H^+$ stretch is expected to be very broad and cannot be detected with certainty. To detect it, we used the following method. After completion of the reaction, gaseous N_2O was removed by evacuation. The cell was sealed and heated to $100\text{ }^\circ\text{C}$ for 5 min. The IR spectrum shows the emergence of a weak spectrum of gaseous N_2O from the desorbed N_2O . It should be noted that the broad band of the bridged proton of the free $H\{F_{11}\}$ acid at 1616 cm^{-1} appeared as well. That is, reaction (1) of N_2OH^+ decomposition takes place.



Partial decomposition of N_2OH^+ should decrease the absorption corresponding to the $O-H^+$ stretch. This allows us, by calculating the difference in the spectra before and after heating, to detect the absorption corresponding to the $O-H^+$ stretch with positive intensity, whereas the absorption corresponding to the H-vibrations of $H\{F_{11}\}$ will have negative intensity.

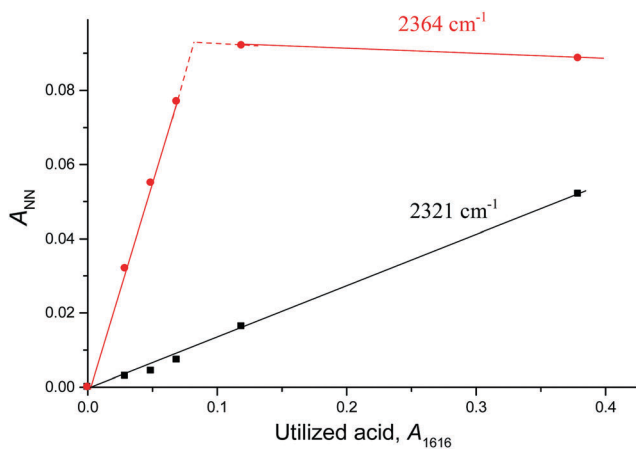


Fig. 4 Dependences of the intensity of the bands of ν_{NN} from cations $N_2OH^+_b$ (at 2321 cm^{-1}) and $N_2OH^+_c$ (at 2364 cm^{-1}) on the absorption of the acid being used (is equal to the decrease in intensity of the free acid at 1616 cm^{-1}).

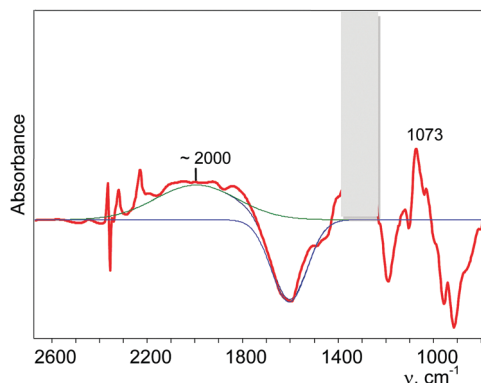


Fig. 5 Determination of the band of the $O-H^+$ stretch of the N_2OH^+ cation (for details see Fig. S10 in ESI[†]).

As shown in Fig. 5 and Fig. S10 (in ESI[†]), $\nu(O-H^+)$ emerges as a broad band at *ca.* 2000 cm^{-1} .

Interaction of NO_2 with the $H\{F_{11}\}$ acid

Interaction of gaseous NO_2 with a thin film of the amorphous acid on the Si windows of the IR cell reactor results in a decreasing absorption band of the bridged proton of the $H\{F_{11}\}$ acid at 1616 cm^{-1} and the appearance of new bands of the formed compounds (Fig. 6). The reaction finished after *ca.* 3 h.

IR spectra of the resulting products do not contain bands of the $NO_2H^+ \cdots L$ type compounds predicted by calculations (Table S3, ESI[†]) but show bands of the stretch vibrations in the frequency region of $2300\text{--}2400\text{ cm}^{-1}$ belonging to the other compounds. One of these bands at 2364 cm^{-1} coincides exactly with that of $N_2OH^+_c$. Moreover, as the reaction of NO_2 with $H\{F_{11}\}$ proceeded, the band of the NN stretch at 2223 cm^{-1} of gaseous N_2O emerged and increased in intensity (Fig. 6, inset). The dependence of the intensity of the band at 2364 cm^{-1} on that of 2223 cm^{-1} is strictly proportional (Fig. 7); this result confirmed the joint formation of $N_2OH^+_c$ and N_2O in the course of the secondary reactions that take place between the initially formed $NO_2H^+_c$ and gaseous NO_2 .

A distinctive band of the second compound at 2334 cm^{-1} is typical in terms of frequency for the NN stretch of the N_2OH^+ cation but did not coincide with that of $N_2OH^+_b$ discussed above. The character of changes in the intensity of this band is manifested in a certain relation with another band in the spectra at 3560 cm^{-1} (Fig. 6) which, without a doubt, belongs to OH stretch vibrations (IR spectra did not show the bands from the OH stretches of the H_3O^+ cation⁴). The dependence of the intensity of the band at 2334 cm^{-1} on that of ν_{OH} at 3560 cm^{-1} is directly proportional (Fig. 8), which means that they belong to one compound. A sample of this compound was obtained when a powder of the $H\{F_{11}\}$ acid (precipitated in liquid HCl during its synthesis) was aged in an atmosphere of NO_2 . At a low partial pressure of NO_2 (*ca.* 0.2 atm) presumably $N_2OH^+_c$ is formed, whereas at a higher partial pressure (*ca.* 0.8 atm) the second compound mainly is formed (Fig. 9a). The only new band detected in the spectrum of the second compound



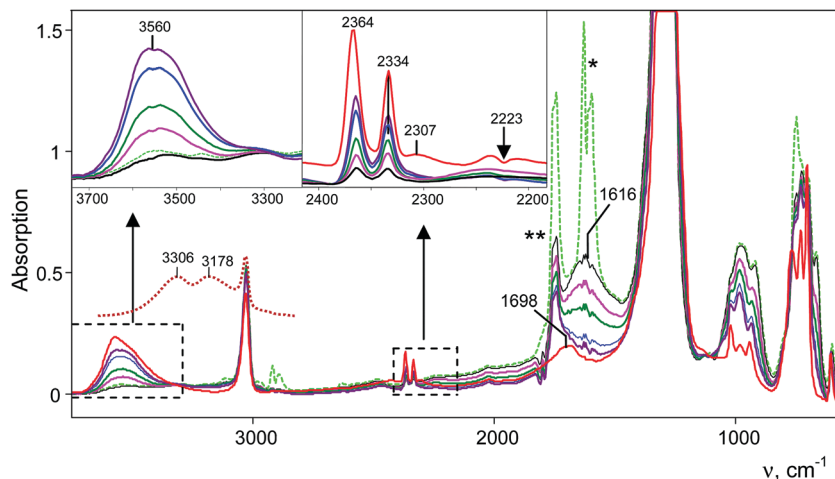


Fig. 6 IR spectra of the reaction products of a gas mixture $\text{NO}_2 + \text{N}_2\text{O}_4$ with the $\text{H}\{\text{F}_{11}\}$ acid. Reaction times are 4 min (green, black curves), 3 h (purple curve) and 24 h (red curve). Spectra are shown without (green curve) and with digital subtraction (full for N_2O and partial for N_2O_4) of the spectrum of the gaseous mixture (dark purple curve). The red spectrum was registered after vacuum removal of the gaseous mixture. $\nu_{\text{as}}\text{NO}_2$ of NO_2 is marked with *, and ν_9 of N_2O_4 is marked with **. ⁴⁵ The spectrum of $\text{H}_3\text{O}^+\{\text{F}_{11}^-\}$ in the frequency region of OH stretches is given for comparison (dotted brown curve).

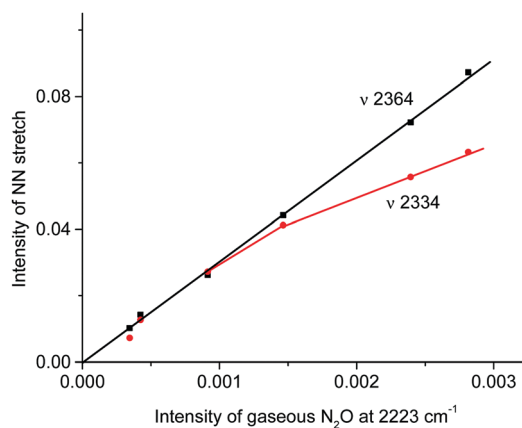


Fig. 7 Dependences of the intensity of the $\text{N}\equiv\text{N}$ stretch of the N_2OH^+ cation on the intensity of the band at 2223 cm^{-1} of the formed gaseous N_2O .

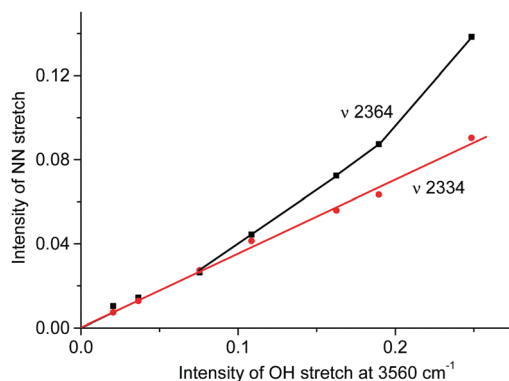


Fig. 8 Dependences of intensity of the $\text{N}\equiv\text{N}$ stretch of the N_2OH^+ cation on the intensity of the band of the OH stretch at 3560 cm^{-1} .

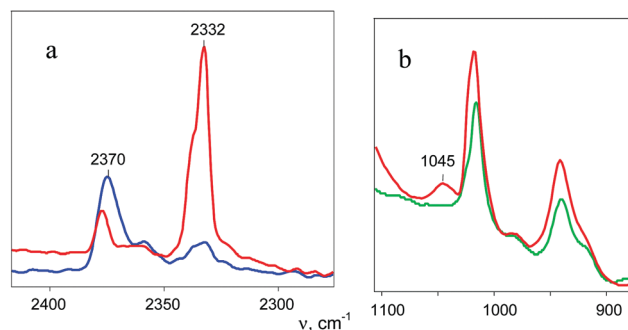


Fig. 9 ATR IR spectra of $\text{N}_2\text{OH}^+\{\text{F}_{11}^-\}$ (blue curve) and $\text{N}_2\text{OH}_{\text{free}}^+\{\text{F}_{11}^-\}$ (red curve) in comparison with the spectrum of the salt $\text{Cs}\{\text{F}_{11}^-\}$ (green curve), which allowed identification of the $\text{N}-\text{O}(\text{H}^+)$ stretch at 1045 cm^{-1} for $\text{N}_2\text{OH}_{\text{free}}^+$.

is at 1045 cm^{-1} , which is common for the $\text{N}-\text{O}(\text{H})$ stretch frequency (Fig. 9b and Table S2, ESI[†]).

This sample was placed on the bottom of the IR cell reactor, and after addition of a drop of water, the cell was sealed. The IR spectra registered the appearance of the absorption pattern of gaseous N_2O . Thus, the second compound is the salt of the N_2OH^+ cation with a free OH bond (further denoted as $\text{N}_2\text{OH}_{\text{free}}^+$), which is decomposed by water with N_2O elimination.

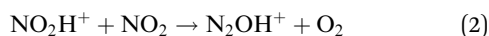
Finally, the third band in the frequency range of the NN stretch appears at 2307 cm^{-1} after long aging of the sample under an atmosphere of NO_2 (more than 24 h, Fig. 6). We propose that it emerges due to water vapor penetration. We verified this idea by introducing water vapor into the IR cell along with the $\text{N}_2\text{OH}^+\{\text{F}_{11}^-\}$ salt and observed rapid disappearance of the bands of the NN stretches of the N_2OH^+ and $\text{N}_2\text{OH}_{\text{free}}^+$ cations, but the band at 2307 cm^{-1} persisted and even increased in intensity (Fig. S11 in ESI[†]). This finding indirectly confirms the affiliation of this band with the hydrated species.



Discussion

Comparison of the empirical spectra of N_2OH_b^+ and N_2OH_c^+ cations (Table 1) with the calculated spectra (Table S2, ESI†) shows that these cations belong to the $L_1\text{-H}^+\cdots L_2$ type, where $L_1 = \text{N}_2\text{O}$ and $L_2 = \{\text{F}_{11}^-\}$ anion with “b” and “c” basic sites. These empirical spectra show the greatest congruence with those calculated for the $\text{N}_2\text{OH}^+\cdots\text{Kr}$ and $\text{N}_2\text{OH}^+\cdots\text{Xe}$ solvates (Table S2, ESI†); in particular, the $\nu_{\text{N-O}}$ frequency almost coincides with that of $\text{N}_2\text{OH}^+\cdots\text{Kr}$ (Fig. 2). This result implies that an “effective” PA of $\{\text{F}_{11}^-\}$ in the solid $\text{N}_2\text{OH}^+\{\text{F}_{11}^-\}$ salt is close to that of the Kr atom. Moreover, the positive charge and electron density redistribution over the $\text{N}\equiv\text{N-O}$ group of the $\text{N}_2\text{OH}^+\cdots\text{Kr}$ cation, as well as the geometric parameters of these groups, determined by means of calculations, should be very close to those of N_2OH_b^+ and N_2OH_c^+ . Thus, these cations can be described as having the NNO angle close to 180° with the triple $\text{N}\equiv\text{N}$ (*ca.* 1.001 Å) and single $\text{N-O(H}^+)$ bonds (*ca.* 1.252 Å) in accordance with the N oxide valence formula $\text{N}\equiv\text{N}^+\text{-OH}$. On the other hand, the O–H stretch at *ca.* 2000 cm^{-1} indicates strong H-bonding with the $\{\text{F}_{11}^-\}$ anion having the positive charge mainly on the H atom (Scheme 1).

Attempts to protonate NO_2 led to an unexpected result: the spectrum of the cation radical $\text{NO}_2\text{H}^{*\dagger}$ predicted by calculations (Table S3, ESI†) is not registered, but the spectrum of N_2OH^+ cations appeared. Obviously, there is a rapid transition from NO_2H^+ to the N_2OH^+ cation, which can only take place *via* reaction (2)

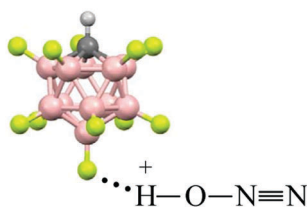


because the formation of other nitrogen oxides was not registered by IR spectroscopy either in the solid phase or in the gas phase. Unfortunately, O_2 generated by reaction (2) is not detected by IR spectroscopy. Eqn (2) is suggestive of the formation of an intermediate: the protonated dimer of nitrogen dioxide, $\text{N}_4\text{O}_2\text{H}^+$. This cation can also be formed by the direct

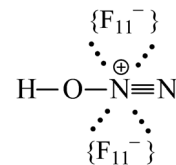
Table 1 Some frequencies of N_2OH^+ cations in solid phases with the $\{\text{F}_{11}^-\}$ counter ion

Cation	ν_{OH}	ν_{NN}	ν_{NO}	δ_{NOH}
N_2OH_b^+	~2000	2321	1073	^a
N_2OH_c^+	~2000	2364	1060	^a
$\text{N}_2\text{OH}_{\text{free}}^+$	3560	2334	1045	1698

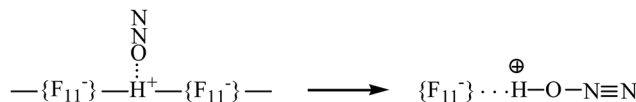
^a Not identified.



Scheme 1 Representative structure of the N_2OH_c^+ cation in its salt with the $\{\text{F}_{11}^-\}$ anion.

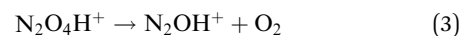


Scheme 2 Schematic presentation of $\text{N}_2\text{OH}_{\text{free}}^+$ in its salt with the $\{\text{F}_{11}^-\}$ anion.



Scheme 3 Illustration of N_2O physically adsorbed by the surface Brønsted centers of the $\text{H}\{\text{F}_{11}\}$ acid (left), followed by the proton transfer to N_2O .

protonation of N_4O_2 , which is present in amounts comparable with those of NO_2 in the gaseous mixture. Unstable $\text{N}_4\text{O}_2\text{H}^+$ further decomposes into N_2OH^+ in accordance with eqn (3)



It was a surprise that one of the two N_2OH^+ cations formed in reactions (2) or (3) is $\text{N}_2\text{OH}_{\text{free}}^+$ with a free OH group, which is not H-bonded to the $\{\text{F}_{11}^-\}$ anion. This means that $\text{N}_2\text{OH}_{\text{free}}^+$ exactly matches the N oxide valence formula $\text{N}\equiv\text{N}^+\text{-OH}$ with the positive charge located on the central N atom. The stretch O–H frequency of $\text{N}_2\text{OH}_{\text{free}}^+$ is higher (3560 cm^{-1}) than that of the free cation in vacuum, both calculated (3332 cm^{-1}) and empirically determined (3331 cm^{-1}).^{12,13} This means that the interaction of $\text{N}_2\text{OH}_{\text{free}}^+$ with the neighboring $\{\text{F}_{11}^-\}$ anions is purely ionic and proceeds *via* the N atom (Scheme 2) leading to polarization of the OH group and an increase in its stretch frequency so much that it even exceeds the value corresponding to naked N_2OH^+ in vacuum. Thus, $\text{N}_2\text{OH}_{\text{free}}^+$ is an unusual representative of a pure Lewis acid with a covalent OH group.

Cation radical $\text{NO}_2\text{H}^{*\dagger}$, formed in the first step of NO_2 protonation with $\text{H}\{\text{F}_{11}\}$, according to calculations (Table S5, ESI†), is stable. Nevertheless, as experiments showed, it has high reactivity and quickly reacts with the next NO_2 molecule (eqn (2)) forming an unstable intermediate, $\text{N}_2\text{O}_4\text{H}^+$. According to calculations, the instability of $\text{N}_2\text{O}_4\text{H}^+$ is caused by extension of the N–N bond up to 2.247 Å. The simplest route of its decomposition is formation of the $\text{HNO}_3\text{-NO}^+$ solvate (Fig. S4, S5 and Table S5 in ESI†). In contrast, the experiment shows that decomposition of $\text{N}_2\text{O}_4\text{H}$ proceeds *via* eqn (3) to $\text{N}_2\text{OH}^+ + \text{O}_2$.

The fact that there is a proportionality between the amount of the formed N_2OH_c^+ and gaseous N_2O (Fig. 2) indicates the existence of an equilibrium $\text{N}_2\text{OH}_c^+\{\text{F}_{11}^-\} \rightleftharpoons \text{N}_2\text{O} + \text{H}\{\text{F}_{11}\}$, which, however, is absent between $\text{N}_2\text{OH}_{\text{free}}^+$ and gaseous N_2O . That is, $\text{N}_2\text{OH}_{\text{free}}^+$ is formed only through $\text{N}_2\text{O}_4\text{H}^+$ decomposition.

Conclusion

Gaseous N_2O and NO_2 are protonated under ambient conditions with the strongest known solid superacid, $\text{H}\{\text{F}_{11}\}$. N_2O is attached



to the H atom of the polymeric $(\text{H}\{\text{F}_{11}\})_n$ acid at the first stage *via* physical adsorption without breaking the bridge H-bond and proton transfer to the N_2O molecule (Scheme 3, left). The adsorbed N_2O molecules are not desorbed in vacuum at room temperature, but are easily detached at elevated temperatures.

The second stage is the breakage of the $-\{\text{F}_{11}\}-\text{H}-\{\text{F}_{11}\}-$ hydrogen bridge and proton transfer to the O atom of N_2O (Scheme 3). The formed N_2OH^+ cation retains a fairly strong H bond with the $\{\text{F}_{11}^-\}$ anion, attaching to its “b” or “c” site (Scheme 1). This compound can be regarded as an asymmetric proton disolvate, $\text{L}_1-\text{H}^+\cdots\text{L}_2$, with $\text{L}_1 = \text{N}_2\text{O}$ and $\text{L}_2 =$ counterion.

Adsorption of NO_2 on the surface of the $\text{H}\{\text{F}_{11}\}$ acid did not reveal the IR absorption pattern of physically adsorbed NO_2 or protonated NO_2 because the cation radical NO_2H^+ , which obviously must be formed, has high reactivity. It quickly interacts with NO_2 forming an unstable intermediate, $\text{N}_2\text{O}_4\text{H}^+$, which decomposes (eqn (3)) forming two types of N_2OH^+ cations. The first one is N_2OH_c^+ with a common H-bonding to the $\{\text{F}_{11}^-\}$ ion. The second one, $\text{N}_2^+\text{OH}_{\text{free}}$, is unusual in that it has a free non-acid OH group with a positive charge localized to the central N atom, which enters into an ionic interaction with anions in the environment (Scheme 2). Thus, if the first N_2OH_c^+ cation is a typical Brønsted superacid, then the second cation, $\text{N}_2^+\text{OH}_{\text{free}}$, is a strong Lewis acid that is formed only as a result of a chemical reaction, but not as a result of the sorption or desorption interaction.

The present work shows that N_2O , just as CO studied earlier, during protonation by the $\text{H}\{\text{F}_{11}\}$ acid, cannot form a symmetric proton disolvate of the $\text{L}-\text{H}^+-\text{L}$ type in the solid phase. For this reason, the results of another article [ref. 25]—claiming that CO_2 , less basic than either N_2O or CO, forms the stable salt of the proton disolvate under ambient conditions—are questionable, especially because the supporting experimental evidence is not convincing.

Conflicts of interest

There are no conflicts to declare.

Acknowledgements

This work was supported by a grant # 16-13-10151 from the Russian Science Foundation. The authors thank Dr Anton S. Nizovtsev for providing the quantum chemical calculations. The synthesis of $\text{H}(\text{CHB}_{11}\text{F}_{11})$ acid was supported by the Russian Foundation for Basic Research (grant # 16-03-00357).

References

- R. J. Gillespie and G. P. Pez, *Inorg. Chem.*, 1969, **8**, 1233.
- P. J. F. Rege, J. A. Gladysz and I. T. Horvath, *Science*, 1997, **276**, 776.
- E. S. Stoyanov and S. A. Malykhin, *Phys. Chem. Chem. Phys.*, 2016, **18**, 4871.
- M. Nava, I. V. Stoyanova, S. Cummings, E. S. Stoyanov and C. A. Reed, *Angew. Chem., Int. Ed.*, 2014, **53**, 1131.
- F. H. Field and J. L. Franklin, *J. Am. Chem. Soc.*, 1961, **83**, 4509.
- J. A. Burt, J. L. Dunn, M. J. McEwan, M. M. Sutton, A. E. Roche and H. I. Schiff, *J. Chem. Phys.*, 1970, **52**, 6062.
- S. S. Jr, J. K. Kim, L. P. Theard and W. T. Huntress Jr., *Chem. Phys. Lett.*, 1975, **32**, 610.
- F. C. Fehsenfeld, W. Lindinger, H. I. Schiff, R. S. Hemsworth and D. K. Bohme, *J. Chem. Phys.*, 1976, **64**, 4887.
- K. Hiraoka, T. Shoda, K. Morise, S. Yamabe, E. Kawai and K. Hirao, *J. Chem. Phys.*, 1986, **84**, 2091.
- M. Polášek, M. Kaczorowska and J. Hrušák, *Chem. Phys. Lett.*, 2005, **402**, 138.
- C. F. Neese, P. S. Kreynin and T. Oka, *J. Phys. Chem. A*, 2013, **117**, 9899 and references therein.
- T. Amano, *Chem. Phys. Lett.*, 1986, **130**, 154.
- T. Amano, *Chem. Phys. Lett.*, 1986, **127**, 101.
- M. E. Jacox and W. E. Thompson, *J. Chem. Phys.*, 2005, **123**, 064501.
- U. Seeger, R. Seeger, J. A. Pople and P. v. R. Schleyer, *Chem. Phys. Lett.*, 1978, **55**, 399.
- D. Sengupta, R. Sumathi and S. D. Peyerimhoff, *Chem. Phys.*, 1999, **248**, 147.
- J. E. Del Bene, E. A. Stahlberg and I. Shavitt, *Int. J. Quantum Chem., Quantum Chem. Symp.*, 1990, **24**, 455.
- K. Yamashita and K. Morokuma, *Chem. Phys. Lett.*, 1986, **131**, 237.
- J. E. Del Bene and M. J. Frisch, *Int. J. Quantum Chem., Quantum Chem. Symp.*, 1989, **23**, 371.
- G. M. Chaban, N. M. Klimenko and O. P. Charkin, *Izv. Akad. Nauk SSSR, Ser. Khim.*, 1992, **1**, 126.
- J. Grunenberg, R. Streubel, G. Frantzius and W. Marten, *J. Phys. Chem.*, 2003, **119**, 165.
- J. L. M. Martin and T. J. Lee, *J. Chem. Phys.*, 1993, **98**, 7951.
- X. Huang, R. C. Fortenberry and T. J. Lee, *J. Chem. Phys.*, 2013, **139**, 084313.
- M. C. McCarthy, O. Martinez, K. N. Crabtree, V. Lattanzi, S. E. Novick and S. Thorwirth, *J. Phys. Chem. A*, 2013, **117**, 9968.
- S. Cummings, H. P. Hratchian and C. A. Reed, *Angew. Chem., Int. Ed.*, 2016, **55**, 1382.
- A. D. Becke, *J. Chem. Phys.*, 1993, **98**, 5648.
- B. Lee, W. Yang and R. G. Parr, *Phys. Rev. B: Condens. Matter Mater. Phys.*, 1988, **37**, 785.
- S. Grimme, J. Antony, S. Ehrlich and H. Krieg, *J. Chem. Phys.*, 2010, **132**, 154104.
- F. Weigend and R. Ahlrichs, *Phys. Chem. Chem. Phys.*, 2005, **7**, 3297.
- A. V. Marenich, C. J. Cramer and D. G. Truhlar, *J. Phys. Chem. B*, 2009, **113**, 6378.
- M. K. Kesharwani, B. Brauer and J. M. L. Martin, *J. Phys. Chem. A*, 2015, **119**, 1701.
- G. D. Purvis III and R. J. Bartlett, *J. Chem. Phys.*, 1982, **76**, 1910.
- J. P. Foster and F. Weinhold, *J. Am. Chem. Soc.*, 1980, **102**, 7211.
- A. E. Reed, L. A. Curtiss and F. Weinhold, *Chem. Rev.*, 1988, **88**, 899.



- 35 M. J. Frisch, G. W. Trucks, H. B. Schlegel, G. E. Scuseria, M. A. Robb, J. R. Cheeseman, G. Scalmani, V. Barone, B. Mennucci and G. A. Petersson *et al.*, *Gaussian 09, Revision D.01*, Gaussian Inc., Wallingford, CT, 2013.
- 36 E. D. Glendening and F. Weinhold, *J. Comput. Chem.*, 1998, **19**, 593.
- 37 E. D. Glendening and F. Weinhold, *J. Comput. Chem.*, 1998, **19**, 610.
- 38 E. D. Glendening, J. K. Badenhop and F. Weinhold, *J. Comput. Chem.*, 1998, **19**, 628.
- 39 E. van Lenthe, E.-J. Baerends and J. G. Snijders, *J. Chem. Phys.*, 1993, **99**, 4597.
- 40 ADF2016, SCM, Theoretical Chemistry, Vrije Universiteit, Amsterdam, The Netherlands, <http://www.scm.com>.
- 41 C. F. Guerra, J. G. Snijders, G. te Velde and E. J. Baerends, *Theor. Chem. Acc.*, 1998, **99**, 391.
- 42 G. te Velde, F. M. Bickelhaupt, E. J. Baerends, C. Fonseca Guerra, S. J. van Gisbergen, J. G. Snijders and T. Ziegler, *J. Comput. Chem.*, 2001, **22**, 931.
- 43 D. Feller, *J. Comput. Chem.*, 1996, **17**, 1571.
- 44 K. L. Schuchardt, B. T. Didier, T. Elsethagen, L. Sun, V. Gurumoorthi, J. Chase, J. Li and T. L. Windus, *J. Chem. Inf. Model.*, 2007, **47**, 1045.
- 45 R. V. St. Louis and B. Crawford Jr., *J. Chem. Phys.*, 1965, **42**, 857.

